XVII[th] World Congress of the International Commission of Agricultural and Biosystems Engineering (CIGR)

Hosted by the Canadian Society for Bioengineering (CSBE/SCGAB)
Québec City, Canada June 13-17, 2010

DESIGN AND MANUFACTURE OF A NEW AND SIMPLE MECHANISM FOR TRANSMISSION OF POWER BETWEEN CROSSOVER SHAFTS UP TO 135 DEGREES FOR FARM MACHINERY

M. YAGHOUBI[1], S.S. MOHTASEBI[1], A. JAFARI[1], H. KHALEGHI[1]

[1] M. YAGHOUBI Department of Agricultural Machinery Engineering, Faculty of Engineering and Technology, University of Tehran, Iran, yaghoub@ut.ac.ir.
[1] S.S. MOHTASEBI, Mohtaseb@ut.ac.ir.
[1] A. JAFARI, Jafarya@ut.ac.ir.
[1] H. KHALEGHI, Hamid_khaleghi66@yahoo.com.

CSBE100240 – Presented at Section III: Equipment Engineering for Plant Production Conference

ABSTRACT In this paper we present a new mechanism developed for transmission of power between crossover shafts. The mechanism consists of one drive shaft and one driven shaft, 6 guide arms, and 3 connecting arms. In this mechanism, the angle between the input- and output shafts (crossover shafts) can be varied up to 135 degrees, while the velocity ratio between input- and output shafts remains constant and equal for all angle of rotation, and the maximum input speed is 2000 rpm. We first present the kinematics diagrams and then the equations of design. Simulation results using Visual NASTRAN, Autodesk Inventor Dynamic, and COSMOS motion software showed that this mechanism could transmit constant velocity ratios at all angles formed between the shafts. Finally, tension analysis of the mechanism at 2000 rpm and input shaft torque of 1000 N.m, using ANSYS software, showed that the highest tension occurred in the connecting arms.

Keywords: Kinematics diagram, Tension analysis, Visual Nastran, COSMOS, ANSYS.

Nomenclature	
a (m)	Horizontal length of connecting arm.
a_L (m)	Linear acceleration of Point B.
B (m)	Joint of guider and connecting arm.
b (m)	Length of slope of connecting arm.
C (m)	Height of branch shafts
C-C (m)	Rotating shaft of connecting arm.

f(α) (rad)	Variable angle between shaft axis and guider arm.
G (m)	Conflict value.
K (m)	Length of shaft.
k	Rotating axis of entrance shaft.
L (m)	Length of guider arm.
m (m)	Width of connecting arm.
R (m)	Radius of Shaft
r (m)	Radius of branches.
R_m (m)	Shortest vertical distance assumed between point B and entrance shaft.
s	Rotating center of connecting arm.
t (m)	Thickness of connecting arm.
V (m^3)	Space (volume) occupied by mechanism during rotation.
v (m/s)	Linear velocity of point B.
α (rad)	Deviation angle between entrance shaft and C-C axis.
β (rad)	Slope of connecting arm with respect to the vertical line on its surface.
γ (rad)	Rotating angle of entrance shaft.
$\dot{\gamma}$ (rad/s)	Angular velocity of entrance shaft.
$\ddot{\gamma}$ (rad/s^2)	Angular acceleration of entrance shaft.
θ (rad)	Rotating degree of connecting arm.
$\dot{\theta}$ (rad/s)	Angular velocity at point B.
$\ddot{\theta}$(rad/s2	Angular acceleration at point B.
Σ (rad)	Angle value of conflict.
Ω (rad)	Angle between the two shafts when the third type of conflict occurs.

INTRODUCTION Currently, several mechanical, pneumatic, hydraulic, and magnetic mechanisms are used to transmit power between two crossover shafts; however, the mechanical type (universal joint) is mostly used in industry due to its low cost (Drevard, 1970). Hooke- and Bendix joints are the two types in common use and are categorized into two types: the Cardan and spherical, which have relative crossover angles of 15 and 45 degrees, respectively. These types of joints are used in equipment with high power transmission; however, the angular velocity of the driven shaft is not constant. This means that the ratio of output velocity to input velocity is not equal at all angles of rotation (Shirkhorshidian, 2004). As this produces a variable velocity ratio in Hooke joints, some researchers tried to design and manufacture joints of constant velocity ratio as explained in the paragraphs that follow. Rzeppa, in 1933, designed a power transmission system that used a ring and shots and which had a constant velocity ratio (Winkler, 1985), besides another simple joint designed by Bendix; these two types of joints have been used the most in automobiles (Dodge, 1943).However, as these two types were not suitable for use in high torque power transmission systems, two Hooke-type universal joints were used in series to overcome this problem (Rzeppa, 1933). For low torque power transmission applications such as in toys and some measurement tools, a mechanism with two contact arms that worked on the homocentric plane principle was used (Shirkhorshidian, 2004). Finally, there are some joints such as Myrad joint, Dodge joint, Lyons joint, Drevard joint, Gilbert joint, James joint, Haruo Mochida joint, Winkler joint and Robert Head joint, which have constant velocity ratios. However, the drawback of these mechanisms is their restricted crossover angle (except for the James mechanism, the others have crossover angles less than 45 degrees) and also some of them take up much space (Dodge., 1943; Drevard., 1970; Myrad., 1935; Contreras., 1972; Falk., 1975; Lynos., 1965; Erdman et al., 1991; Behroozi Lar., 2003; Hojjati., 2000; Haruo., 1982; Winkler., 1985; Head., 1987). The mechanism we propose can be used between two shafts with a crossover angles smaller than 135 degrees. It has six guide arms and three connecting arms. It is dynamically balanced and occupies optimum working space and also its velocity ratio is constant for all crossover angles between the two shafts.

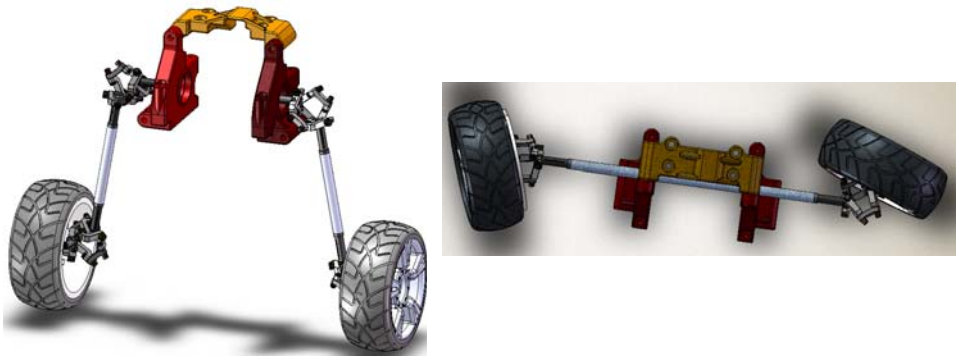

Fig.1. The applications of mechanism on axle of farm machinery.

MATERIAL AND METHODS Fig. 2 shows the kinematics diagram of one part (three links) of this mechanism which is able to transmit motion at an inconsistent velocity ratio and maximum angle of 37.5 degrees (Shirkhorshidian., 2004). Now, if we connect two

similar assemblies of this part to one another it results in a new mechanism with a constant velocity ratio (Fig.3), which, however, is not dynamically balanced.

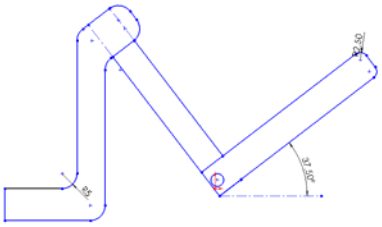

Fig .2. One part of the mechanism.

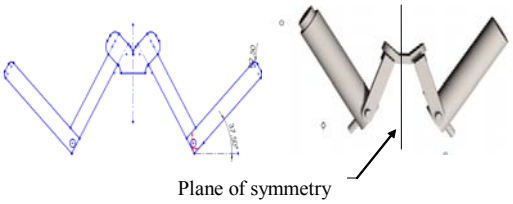

Fig. 3. Two similar parts are combined to produce a new mechanism.

As seen in Fig 3, the intersecting angle of the new mechanism is greater than 75 (37.5×2) degrees.

Fig. 4. A sample of proposed mechanism that can rotate to a crossover angle of 135 degrees.

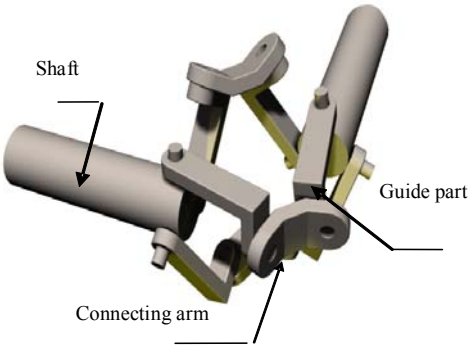

Fig. 5. A schematic of the new mechanism

Because it is not dynamically balanced, this mechanism cannot transmit power satisfactorily. So it had to be redesigned such that its symmetry is preserved in the plane of symmetry for all the angles that may arise with a constant angular velocity ratio.

To balance the mechanism, three connecting arms and six guide arms are used as shown in Figs. 3 and 4. The addition of two extra arms enables the mechanism retain its symmetry about the plane of symmetry. (Fig. 6)

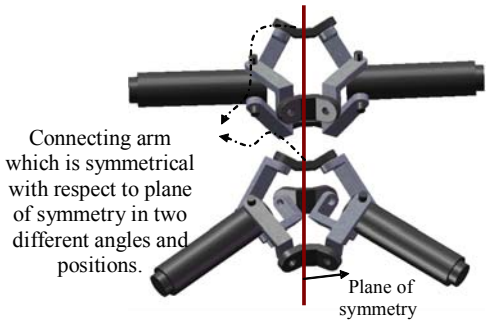

Fig. 6. Preserving symmetry of the mechanism about the plane of symmetry.

Fig. 7. Kinematics diagram of the whole mechanism.

Kinematics analysis of the mechanism Fig. 8 illustrates the kinematics diagram of the mechanism with the two shafts at an angle of 90 degrees to each other. Fig.8 shows the input shaft at a relative angle (f (α)) to the guide arm during rotation. This variable angle is the crucial parameter in analysis of the mechanism, and its measurement, as shown in Fig. 8, is obtained from following equations.

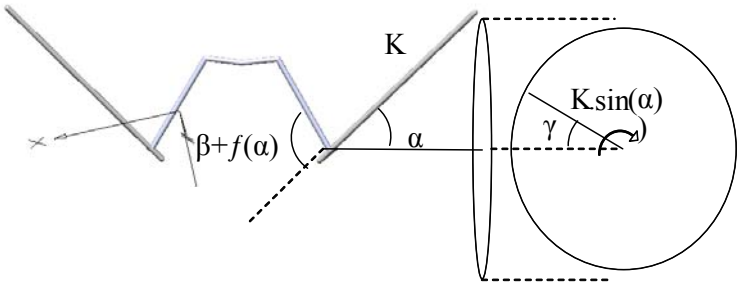

Fig. 8. Relative locus of rotating shaft with respect to guide arms

$$f(\alpha) = \arctan(\sin(\gamma).\tan(\alpha)) \quad (1)$$

Then, the whole of this angle (measured between shaft and guide arm) is equal to β+f(α).

The analysis is carried out on one part of the mechanism for ease of calculation. (Fig.9)

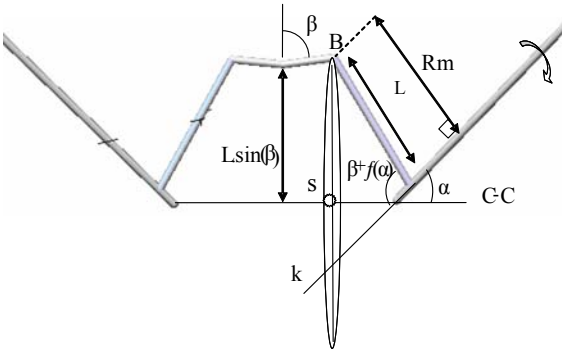

Fig. 9. A simple kinematics diagram of the mechanism

In rotation, the motion of the connecting arm is unsteady. As shown in Fig 9, point B is the intersection of the guide- and connecting arms, and its motion about the C-C axis is

circular with its center at s. Axis k is the axis of the input shaft where the vertical distance between point B and the k axis is equal to Rm. So we have:

$$v = R_m.\gamma^{\bullet} = L.\cos(\beta - \tan^{-1}(\sin(\gamma).\tan(\alpha)).\gamma^{\bullet} \quad (2\text{-a})$$

$$\theta^{\bullet} = \frac{v}{L.\sin\beta} = \frac{\gamma^{\bullet}.\cos(\beta - \tan^{-1}(\sin(\gamma).\tan(\alpha))}{\sin(\beta)} \quad (2\text{-b})$$

$$a_L = v^{\bullet} = \frac{L.\gamma^{\bullet 2}.\cos(\gamma).\tan(\alpha).\sin(\beta - \tan^{-1}(\sin(\gamma).\tan(\alpha)).\sin(\beta)}{1 + (\sin(\gamma).\tan(\alpha))^2 + \gamma^{\bullet\bullet}.\gamma^{\bullet}\cos(\beta - \tan^{-1}(\sin(\gamma).\tan(\alpha)))} \quad (2\text{-c})$$

$$\theta^{\bullet\bullet} = \frac{a_L}{L.\sin\beta} = \frac{\gamma^{\bullet 2}.\cos(\gamma).\tan(\alpha).\sin(\beta - \tan^{-1}(\sin(\gamma).\tan(\alpha)).\sin(\beta)^2}{1 + (\sin(\gamma).\tan(\alpha))^2 + \gamma^{\bullet\bullet}.\gamma^{\bullet}\cos(\beta - \tan^{-1}(\sin(\gamma).\tan(\alpha)))} \quad (2\text{-d})$$

Relations between the components of the mechanism

The space (volume) occupied by the mechanism From Fig. 10, it is seen that for any crossover angle between the two shafts, the guide arms occupy a constant space during rotation, which is shown in color in Figs. 20 and 21. This space is central to the design of the mechanism as it determines the working space required.

$$V = \frac{\pi}{3}.a.(2.L^3.\sin(\beta) + 2.\sin(\beta).(L^3 - (L-a)^3) + 3.b.(L-a)^2) \quad (3)$$

Thus, the space occupied by the mechanism is equal to the value obtained from Equation (3).

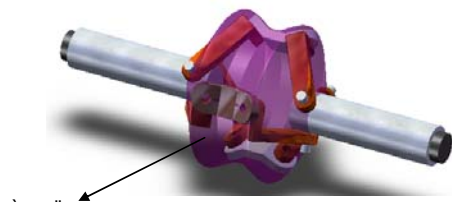

Fig. 10. Space (volume) occupied by the

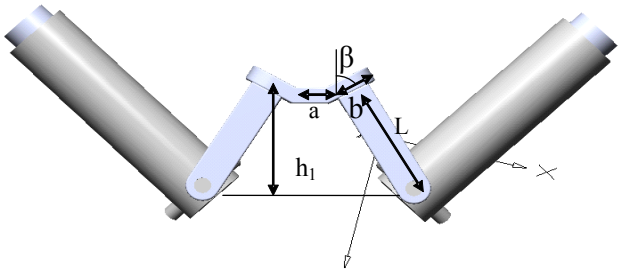

Fig. 11. Schematic of component parameters of the mechanism.

Conflict of arms during rotation Because of the configuration of the arms, conflict arises between them at angles greater than the acceptable values. Generally there are three types of conflicts, which are as illustrated as follows:

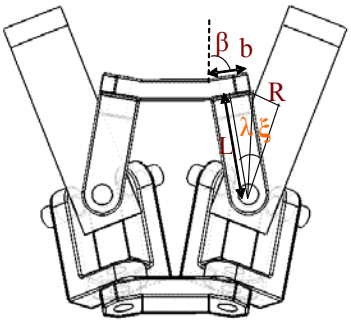

Fig. 12. Position of arms in the first type of conflict.

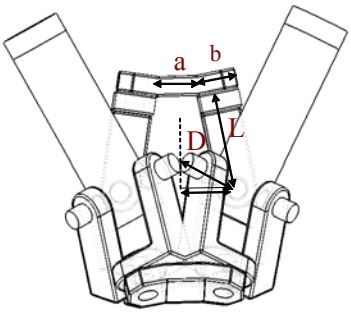

Fig. 13. Position of arms in the second type of conflict.

From Fig 12, it is evident that the guide arm conflicts with the shaft due to the higher crossover angle. This problem is avoided when the following equations are satisfied:

$$\begin{cases} \alpha \le (90 + \beta - (\lambda+\xi)) \\ \lambda = \arctan(\dfrac{b}{2L}) \quad , \quad \xi = \arcsin(\dfrac{R}{\sqrt{L^2 + \dfrac{b^2}{4}}}) \end{cases} \tag{4}$$

In Fig 13, two of the three branches of shafts conflict with each other. This problem is avoided when the following equations are satisfied:

$$D = R + C = \frac{(L + \frac{b}{2}).\sin(\beta) + r.\cos(\alpha)}{\cos(\alpha).\cos(30)} \tag{5}$$

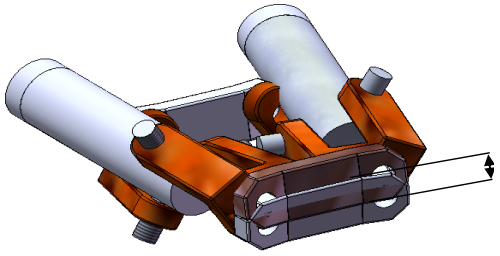

Fig. 14. The third type of conflict.

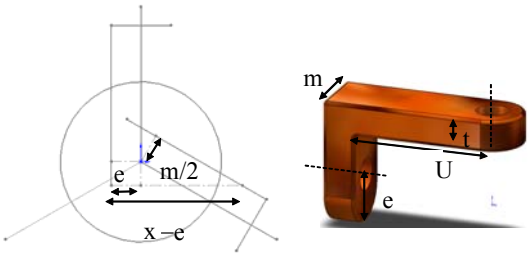

Fig. 15. Mechanism parameters for the third type of conflict.

Due to different velocities of the linkages, at some crossover angles, a conflict as shown in Fig. 14 is possible. To avoid this type of conflict, we should find a relation based on acceptable slope angle, length, and thickness of the linkage. By solving the equation for the conditions shown in Fig. 15, we obtain the conflict value. In this design, the conflict value must be negative. The implication is that when the conflict value is zero, it

represents the starting point of conflict and if, for example, the conflict value is -4, it indicates that the closest point of conflict of the two guide links is 4 mm.

Fig 15 shows that the conflict value at the crossover angle (180-2β), that is, the angle between the two shafts is equal to the thicknesses of the connecting arms. This causes the two linkage components in conflict to overlap exactly over each other. Therefore, to obtain the conflict value, we have to find the value of Σ angle and subtract it from the (180-2β). From the related figure, we obtain following relations:

$$\frac{x}{m/2} = \frac{e + \dfrac{m}{2.\tan(60)}}{\dfrac{m}{2.\tan(60)}}$$

Now, if we have such a relation we can obtain the value of Σ:

$$\sum = \arcsin\left(\frac{e.(1 + \tan(60) - G + m/2)}{2.(U - t)}\right)$$

Thus, the angle formed between the two shafts in conflict is equal to:

$$\begin{cases} \Omega = (180 - 2\beta - 180.\Sigma/2\pi) \\ \Omega/2 \le \alpha \end{cases} \tag{6}$$

RESULTS

Simulation and results The greatest advantage of the proposed mechanism is its constant angular velocity ratio during rotation. As was shown in Fig. 6, there is symmetry in all the angles, so the mechanisms have constant velocity ratio. Simulations carried out using powerful software such as COSMOS Motion, Visual Nastran, and Autodesk Inventor also confirm this claim and their results are shown in Fig. 16.

The simulations shown in Fig. 16 are (a) with variable velocity of f(x) and in Fig. 16 (b) and (c) at steady velocity of π/2 rad/s. The output value is negative because of the positions of the input- and output axes in the Cartesian coordinates which are reversed in simulation. As shown in Fig 17, the response time at the step input of 2000 rpm is about 0.001 s, which is negligible.

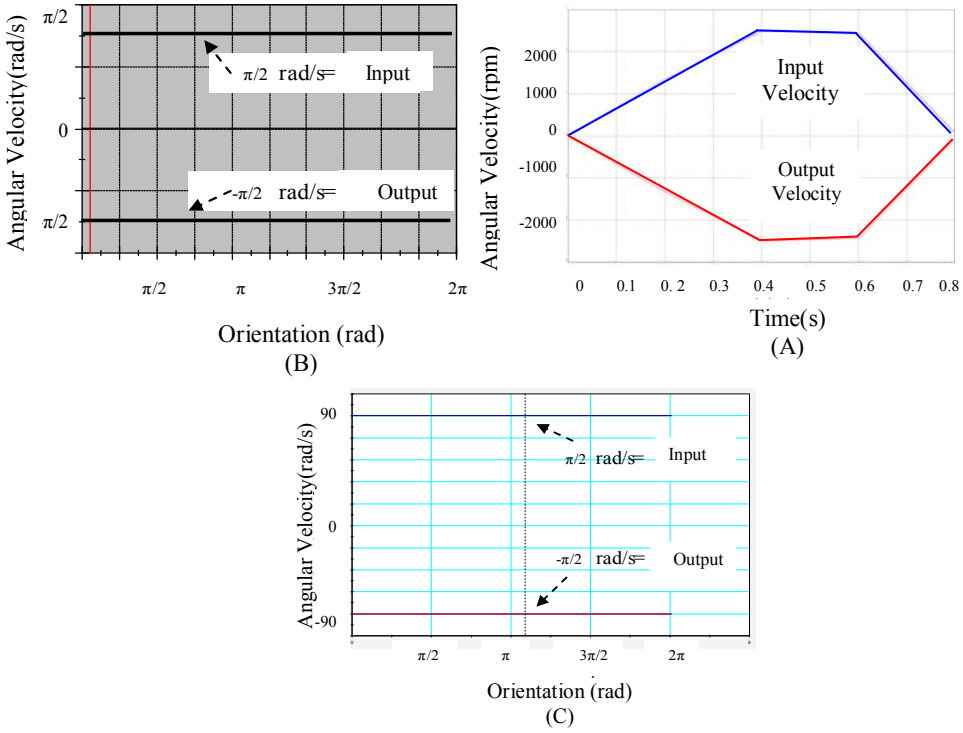

Fig. 16. Comparisons between input- and output velocities of the mechanism: A) Simulation by Autodesk Inventor software. B) Simulation by COSMOS Motion software. C) Simulation by Visual Nastran software. [Note: Blue line: Input velocity, Red line: Output velocity]

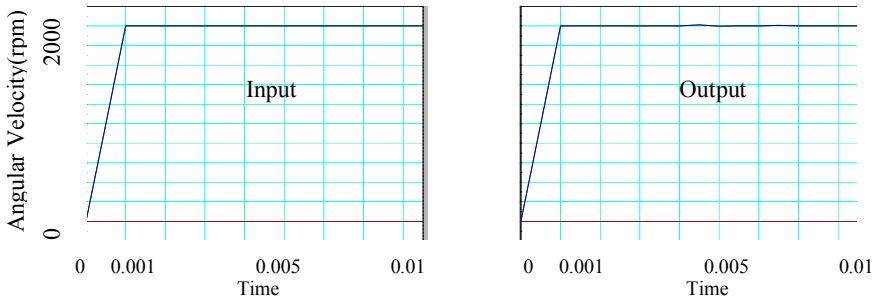

Fig. 17. Simulation results for step input of 2000 rpm; the response time for output is about 0.001 sec.

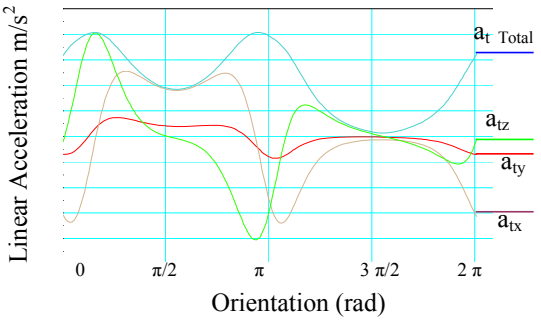

Fig. 18. Acceleration of connecting arm in three dimensions and also maximum acceleration (Absolute Acceleration).

As the mechanism was designed for a mechanism crossover angle of 135 degrees, the simulation of mechanism was carried out at this angle. Further, it is observed that the higher the crossover angle, the greater the variations of force, velocity, and acceleration in the linkages. Variable acceleration might cause jerking, but Fig. 18 shows that the angle of the slope for acceleration of the connecting arms is 135 degrees and not 90 degrees; therefore, no jerk takes place in the system.

Transmission capacity The mechanism was analyzed using ANSYS software and the results of the simulation are shown in Fig. 19.

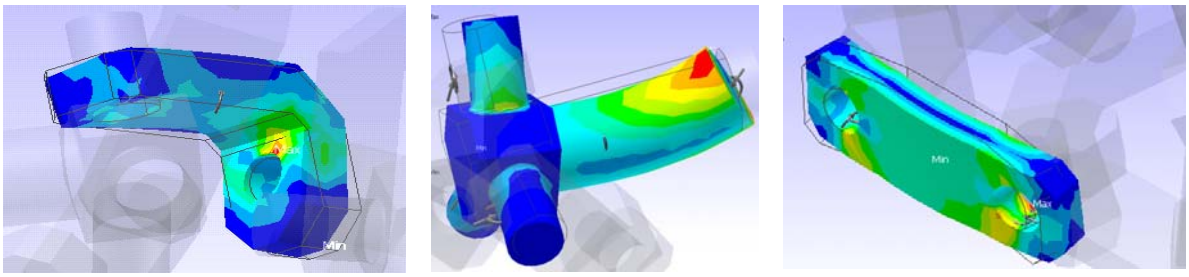

A B C

Fig. 19. Simulation results using ANSYS software: A): Tension in guide arm. B): Tension in shaft. C): Tension in connecting arm.

The analysis of tension in the mechanism's components was carried out at 2000 rpm and 1000 N/m for the input shaft. As shown in Fig. 19, this mechanism is made of alloy steel and has a shaft diameter of 30 mm, guide component diameter of 15mm, and connecting arms' diameters each of 10 mm. The result of safety factor was 1.7. The simulation results reveal that the maximum tension occurs in the connecting arm, as shown in Fig 20.

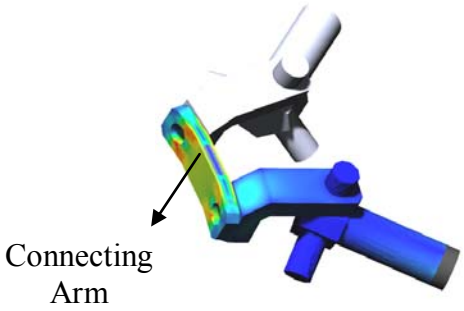

Fig. 20. Tension in all the parts of the mechanism as visualized by Nastran software.

CONCLUSION The proposed mechanism has a constant velocity ratio and transmits power between two crossover shafts at angles formed up to 135 degrees. Using Ansys and Visual Nastran software, the maximum tension was found to occur in the connecting arm. The mechanism transmits the power without vibration and on altering the dimensions of its components it can transmit much more power.

REFERENCES

Behroozi Lar. M. 2003. The Principles of Agricultural Machinery Design (translation).Islamic Azad publication (in Persian).

Contreras. G. E 1972. Universal joint. United State Patent. Patent No.3, 633,044.

Dodge. A. Y. 1943. Universal joint. United State Patent .Patent No. 2, 322, 5.

Drevard. E. M. 1970. Universal joint. United State Patent .Patent No. 3,613,396

Erdman. G. Sandor. G. N .1991. Mechanism Design. Printice Hall publication.

Falk. J. B. 1975. Universal joint. United State Patent .Patent NO 3,924,420

Haruo. M. 1982. Universal joint. United State Patent .Patent NO 4,365,488

Head. R. 1987. Universal joint. United State Patent .Patent NO 4,695,227.

Hojjati. M. H. 2000. Design of Machine. University of Mazandaran publication (in Persian).

Lynos. J. M. 1965. Universal joint. United State Patent .Patent NO 3,178,907

Myrad. F. E 1935. Universal joint. United State Patent .Patent NO 2,026,244

Rzeppa. A.H. 1933. Universal joint. United State Patent .Patent NO 1, 916,442

Shirkhorshidian. A. 2004. Design of mechanisms for designer and machine makers. Nashretarrah publication. (in Persian).

Winkler. O. 1985. Universal joint. United State Patent .Patent NO 4,511,345